Unsteady Axisymmetric Flows of a Liquid Draining from a Circular Tank

C. Y. CHOW* AND W. M. LAI†
Rensselaer Polytechnic Institute, Troy, N. Y.

The problem of unsteady axisymmetric flows of a liquid draining from a circular cylindrical tank, with a centrally located drain at the flat bottom and nonlinear boundary conditions at the free surface, is studied. The liquid is assumed to be inviscid and incompressible with a constant density. Initially, the liquid is at rest. Subsequently, this is drawn from the drain with a constant discharge. Numerical solutions of the free surface shape and the residual volume are obtained at small time intervals from the initial condition until the inception of dip formation on the free surface. Parametric studies of the geometry, the Froude number and the Weber number were made. Results checked reasonably well with some published experimental data.

Nomenclature

$A_m^{(n)}$ = coefficients defined in Eq. (19)
a = radius of the drain
$\bar{a}$ = drain radius ratio a/r_o
B_o = Bond number $\rho g(2r_o)^2/T$
$\mathrm{B}_m^{(n)}$ = coefficients defined in Eq. (19)
C = a constant appearing in Eq. (2)
$f^{(n)}(\xi)$ = functions of ξ [see Eqs. (23) and (24)]
F = Froude number $U^2/(gr_o)$
F_{cr} = critical Froude number $Q_c/(g'h_c^5)^{1/2}$
F_v = Froude number used by Ref. 3, $V_m^2/(2ga)$
g = gravitational acceleration
g' = effective gravitational acceleration $g(\rho_2 - \rho_1)/\rho_2$
$h(\xi, \tau)$ = shape of the free surface
h_c = central height of the liquid at critical flow
h_s = initial height of the liquid in the tank
h_w = height of the free surface on the wall
$h^{(n)}$ = terms of expansion of $h(\xi, \tau)$ on τ defined by Eq. (10)
H_s = initial height ratio h_s/r_o
$H(0, \tau)$ = center height ratio $h(0, \tau)/r_o$
H_c = critical height ratio h_c/r_o
H_w = dimensionless height of the free surface on the wall h_w/r_o
$J_0(k)$ = Bessel function of the zero order
$J_1(k)$ = Bessel function of the first order
k = constant defined by Eq. (18)
k_m = positive mth root of $J_1(k_m)$
Q = constant rate of discharge through the drain
Q_c = critical rate of discharge
r, z = cylindrical coordinates
r_o = radius of the tank
t_c = critical time
t = time
$\bar{t}$ = time parameter $t/(\rho r_o^3/T)^{1/2}$
T = surface tension
$u_m(\xi)$ = orthonormalized functions of ξ defined by Eq. (25)
U = constant discharge velocity through the drain
$v_m(\xi)$ = functions of ξ [see Eqs. (23) and (24)]
V_m = average velocity of the liquid in the tank $U\bar{a}^2$
W = Weber number $r_o\rho U^2/T$
W_e = Weber number used in Ref. 1, $2\rho r_o V_m^2/T$
ξ, η = dimensionless cylindrical coordinates $\xi = r/r_o$, $\eta = z/r_o$
Φ = velocity potential
π = pi
$\varphi = \varphi(\xi, \eta, \tau)$ = dimensionless velocity potential Φ/Ur_o
$\varphi^{(n)}$ = dimensionless velocity potentials defined by Eqs. (12) and (13)
$\varphi^{(n)}(\xi, \eta)$ = dimensionless velocity potentials defined by Eq. (9)
τ = dimensionless time $tUa^2/(h_s r_o^2)$
τ_c = dimensionless time at critical flow
ρ = density of the liquid
ρ_1, ρ_2 = densities of the respectively lower and upper fluid in a two-layer stratified fluid system

Received September 13, 1971; revision received March 23, 1972.
Index category: Hydrodynamics.
* Graduate Assistant
† Associate Professor of Mechanics.

I. Introduction

THE problem of unsteady axisymmetrical flow of an incompressible inviscid fluid, draining from a circular cylindrical tank, has been studied by a number of authors. Saad and Oliver[2] analyzed the problem with linearized boundary conditions on the free surface. Recently, Easton and Catton[1] published some numerical results with the nonlinear boundary conditions used at the free surface. In both cases, the fluid contained is assumed to be with drawn suddenly at a constant rate through a drain located at the center of the tank bottom. The free surface is initially at rest and taken to be flat.

The results given in Ref. 1, include three figures which show 1) the effect of the initial height (for small values) on the center height history, 2) the free surface shapes at three different instants, and 3) a comparison of results with some experimental data. However, the peculiar shapes of the first two curves make the results far from convincing. The present writers study the same problem and use the same fluid model (incompressible and inviscid). We are also interested in quantitative results to find the time elapsed until the free surface reaches the drain. Similarly as in Ref. 1, we equally enforce the nonlinear boundary conditions at the free surface. Yet, the method used in the present study is quite different. This includes notably the nondimensionalization and the application of the Gram-Schmidt orthonormalization scheme to determine some of the coefficients in the governing equation. Moreover, we have obtained significantly different results as compared with those of Ref. 1. Our results check reasonably well with the published experimental data, not only qualitatively but also quantitatively. It is the writers' opinion that the present paper gives 1) good estimates of the critical time, the critical height, and the residue volume of a cylindrical tank during liquid withdrawal and 2) a clear design guide provided through the parametric study discussed later.

II. Governing Equations

In terms of the dimensionless variables and parameters, defined in the Nomenclature (also, see Fig. 1), the governing differential system is, with subscripts denoting differentiation

$$\varphi_{\xi\xi} + \xi^{-1}\varphi_\xi + \xi_{\eta\eta} = 0 \quad \text{in Domain D} \tag{1}$$

$$\varphi_\tau + [0.5(\varphi_\xi^2 + \varphi_\eta^2) - (1 + h_\xi^2)^{-1.5}(h_{\xi\xi} + \xi^{-1}h_\xi + \xi^{-1}h_\xi^3)W^{-1} + hF^{-1}]H_s\bar{a}^{-2} = C \text{ (a constant)} \quad \text{at } \eta = h(\xi, \tau) \tag{2}$$

$$h_\tau = (\varphi_\eta - \varphi_\xi h_\xi)H_s\bar{a}^{-2} \quad \text{at } \eta = h(\xi, \tau) \tag{3}$$

$$\varphi_\xi(0,\eta,\tau)=0 \quad \text{for } \eta\geqq 0,\ \tau\geqq 0 \tag{4}$$

$$\varphi_\xi(1,\eta,\tau)=0 \quad \text{for } H_w(\tau)\geqq\eta\geqq 0,\quad \tau\geqq 0 \tag{5}$$

$$\varphi_\eta(\xi,0,\tau)=\begin{cases}0 & \tau<0\\ -1 & \tau\geqq 0\end{cases} \quad \text{for } 0\leqq\xi<\bar{a} \tag{6}$$

$$\varphi_\eta(\xi,0,\tau)=0 \quad \text{for } \tau\geqq 0,\quad \bar{a}<\xi\leqq 1 \tag{7}$$

and

$$\varphi(\xi,h(\xi,0),0)=0 \tag{8}$$

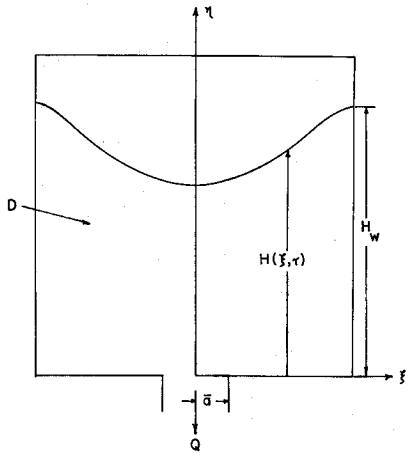

Fig. 1 Schematic of liquid draining from a cylindrical tank.

We note here that Eqs. (2) and (3) are the full nonlinear dynamic and kinematic conditions respectively on the free surface. Equation (6) is the boundary condition at the drain which is enforced with a uniform velocity at all times after the start of the flow. This very condition is used by Saad and Oliver (in their linear theory) and by Easton and Catton. However, the latter further impose an initially uniform velocity on the free surface. It should be pointed out that once the drain condition is prescribed, the axial velocity on the free surface can be determined. This velocity cannot be arbitrarily chosen even at the initial instant. In computation, this assumption probably will not introduce too much error for the cases with the initial height well above the critical height but it seems hard to justify for those cases with the initial height at or near the critical. This point is demonstrated by our results shown in Table 1.

Table 1 Initial rates of central-height ratios of free surfaces, graphical and computed results ($\bar{a}=0.111$, $W_e/\bar{a}=6.0$, $B_o=100.0$)

	Graphical result $h_\tau\|_{\xi=0,\tau=0}$		Computed result
H_s	Present study	Ref. 1	From Eq. (A5)
0.30	−5.2	−4.0	−5.20
0.36	−3.7	−3.0	−3.75
0.42	−2.8	−2.0	−2.83
0.45	−2.5	−1.7	−2.50
0.48	−2.2	−1.5	−2.21

III. Method of Solution

Expanding $\varphi(\xi,\eta,\tau)$ and $h(\xi,\tau)$ into power series of τ, we obtain

$$\varphi(\xi,\eta,\tau)=\varphi^{(0)}(\xi,\eta)+\varphi^{(1)}(\xi,\eta,\tau)+\varphi^{(2)}(\xi,\eta)\tau^2+\dots \tag{9}$$

and

$$h(\xi,\tau)=h^{(0)}(\xi)+h^{(1)}(\xi)\tau+h^{(2)}(\xi)\tau^2+\dots \tag{10}$$

Substituting Eqs. (9) and (10) into Eq. (1), we get

$$\nabla^2\varphi^{(n)}(\xi,\eta)=0,\quad n=0,1,2,\dots \tag{11}$$

Similarly, the conditions at the fixed boundary and at the free surface can be obtained from Eqs. (2–7). The latter gives rise to

$$\varphi^{(1)}=-0.5H_s\bar{a}^{-2}[(\varphi_\xi^{(0)})^2+(\varphi_\eta^{(0)})^2]-h^{(0)}F^{-1}H_s\bar{a}^{-2}+C$$
$$+W^{-1}H_s\bar{a}^{-2}[1+(h^{(0)})^2]^{-1.5}\{h_{\xi\xi}^{(0)}+\xi^{-1}[h_\xi^{(0)}+(h_\xi^{(0)})^3]\}\big|_{\eta=h^{(0)}} \tag{12}$$

$$\varphi^{(2)}=-0.5H_s\bar{a}^{-2}[h^{(1)}(\varphi_\xi^{(0)}\varphi_{\eta\xi}^{(0)}+\varphi_\eta^{(0)}\varphi_{\eta\eta}^{(0)}+\varphi_\eta^{(1)})+\varphi_\xi^{(0)}\varphi_\xi^{(1)}+\varphi_\eta^{(0)}\varphi_\eta^{(1)}+h_1^{(0)}F^{-1}]+0.5H_s\bar{a}^{-2}W^{-1}(1+h_\xi^{(0)})^{-1.5}\{h_{\xi\xi}^{(1)}+\xi^{-1}h_\xi^{(1)}[1+3(h_\xi^{(0)})^2]-3h_\xi^{(0)}h_\xi^{(1)}[1+(h^{(0)})^2]^{-1}[h_{\xi\xi}^{(0)}+\xi^{-1}h_\xi^{(0)}(1+(h_\xi^{(0)})^2)]\}\big|_{\eta=h^{(0)}} \tag{13}$$

$$\varphi^{(3)}=\dots$$

$$h^{(1)}=H_s\bar{a}^{-2}(\varphi_\eta^{(0)}-\varphi_\xi^{(0)}h_\xi^{(0)})_{\eta=h} \tag{14}$$

$$h^{(2)}=0.5H_s\bar{a}^{-2}[h^{(1)}(\varphi_{\eta\eta}^{(0)}-\varphi_{\xi\eta}^{(0)}h_\xi^{(0)})-\varphi_\xi^{(0)}h_\xi^{(1)}-\varphi_\xi^{(1)}h_\xi^{(0)}+\varphi_\eta^{(1)}]_{\eta=h^{(0)}} \tag{15}$$

$$h^{(3)}=\dots$$

Initially, $\tau=0$, the conditions at the free surface are

$$h^{(0)}=H_s \tag{16}$$

and from Eq. (8)

$$\varphi^{(0)}=\varphi^{(0)}(\xi,H_s)=0 \tag{17}$$

These, in conjunction with the fixed boundary conditions, will enable one to solve $\varphi^{(0)}(\xi,\eta)$ and all derivatives $\varphi_\xi^{(0)}$, $\varphi_\eta^{(0)}$, $h_\xi^{(0)}$, etc. Similarly, $\varphi^{(1)}(\xi,\eta)$, $h^{(1)}(\xi),\dots\varphi^{(n)}(\xi,\eta)$, $h^{(n)}(\xi)$ can be computed (results shown later were computed with two terms). Thus, the free surface profile, at τ, can be determined. If the flow has not reached the critical, the entire procedure aforementioned will be repeated.

Solutions of the Laplace Equation in Cylindrical Coordinates

It can be readily verified that the following $\varphi^{(n)}(\xi,\eta)$, where $n=0,1,2,\dots$, satisfy the Laplace equation

$$\varphi^{(n)}(\xi,\eta)=A_o^{(n)}+B_o^{(n)}\eta+\{A^{(n)}[\exp\{-k(H_s-\eta)\}+\exp\{-k(H_s+\eta)\}]-B^{(n)}e^{-k\eta}\}J_o(k\xi) \tag{18}$$

After satisfying the symmetry condition and the fixed wall boundary, Eq.(18) becomes

$$\varphi^{(n)}(\xi,\eta)=A_o^{(n)}+B_o^{(n)}\eta+\sum_{m=1}^{\infty}\{A_m^{(n)}[\exp\{-k_m(H_s-\eta)\}+\exp\{-k_m(H_s+\eta)\}]-B_m^{(n)}\exp(-k_m\eta)\}J_o(k_m\xi) \tag{19}$$

From the drain condition, by expressing $\varphi_\eta^{(0)}(\xi,0)$ into the Dini expansion of $J_o(k_m\xi)$, in $0<\xi<1$, we obtain the constants $B_m^{(n)}$ as

$$B_m^{(n)}=0,\quad n=1,2,3,\dots,\quad m=0,1,2,3,\dots \tag{20}$$

$$B_o^{(0)}=-\bar{a}^2 \tag{21}$$

and

$$B_m^{(n)}=-2\bar{a}J_1(k_m\bar{a})/[k_m^2J_o^2(k_m)],\quad m=1,2,3,\dots \tag{22}$$

The remaining constants $A_m^{(n)}$ are to be determined from the free surface condition. Rearranging Eq.(19), we have

$$\varphi^n(\xi,\eta)-B_o^{(n)}\eta=\sum_{m=0}^{\infty}A_m^{(n)}\{[\exp[-k_m(H_s-\eta)]+\exp[-k_m(H_s+\eta)]]-B_m^{(n)}\exp(-k_m\eta)]J_o(k_m\xi)\} \tag{23}$$

It is noted that, at any specific time τ^*, Eq.(23) depends on ξ only and can be written as

$$f^{(n)}(\xi)=\sum_{m=0}^{\infty}A_m^{(n)}v_m(\xi) \tag{24}$$

To determine the $A_m^{(n)}$ in Eq.(24), we first construct a set of orthonormalized functions $u_m(\xi)$ from $v_m(\xi)$ by the Gram-Schmidt orthonormalization process, i.e.

$$f^{(n)}(\xi)=\sum_{s=0}^{\infty}D_s^{(n)}u_s(\xi) \tag{25}$$

where the coefficients $D_s^{(n)}$ can be obtained from the property of orthogonality or

$$D_s^{(n)} = \int_o^1 f^{(n)}(\xi) u_s(\xi)\, d\xi, \quad n = 0, 1, 2, \ldots \tag{26}$$

It is recalled that $u_m(\xi)$ are constructed, in a form of linear combination, from $v_m(\xi)$. Therefore, the coefficients $A_m^{(n)}$ can be readily determined from the following identity

$$\sum_{m=0}^{\infty} A_m^{(n)} v_m(\xi) = \sum_{m=0}^{\infty} D_m^{(n)} u_m(\xi) \tag{27}$$

A recurrence scheme to compute $A_m^{(n)}$ can be easily constructed in Fortran language for a digital computer and is very economical in computation. By so doing, the difficult task of matrix inversions as required by the method of determining $A_m^{(n)}$ directly from the nonorthogonal system $v_m(\xi)$ is eliminated.

Numerical Solution

Once those coefficients $A_m^{(n)}$ are obtained, the velocity potentials in the entire domain can be computed from Eqs.(19) and (9). The liquid remaining in the tank at successive instances is integrated numerically by the trapezoidal rule on the computed free surface.

All pertinent equations and formulas to obtain the critical flow were programed in Fortran language. The velocity potentials and elevations of the free surface and residual volumes at successive times are computed. The procedure is automatic until the dip formation. Obviously, the success of the numerical solution and the computational economy hinges upon proper choices of time increments $\Delta\tau$. Reviewing the definition of dimensionless time, $\tau = tUa^2/(h_s r_o^2)$, we notice that τ represents the fractional volume of fluid discharged in reference to the originally unperturbed fluid. Since the height of the free surface decreases with time, the foregoing definition suggests that the $\Delta\tau$'s used in later times should be reduced as well. The effect of different choices of initial $\Delta\tau$ is illustrated in Fig. 10. However, the influence of the number of terms of A_m used on the final result of H_c is not significant, which can be seen from Table 2. The required input are H_s, $\bar{a}$, and the initial time increment $\Delta\tau$. The successive $\Delta\tau$'s are generated by an automatic scheme built in the program. The feature of this scheme is described below. First, at any instance, the decrease of the central portion of the free surface is not permitted to be more than 25% of its height; otherwise, the $\Delta\tau$ used is automatically reduced by 50%. Secondly, when the number of time instances reachs 10, 20, 30, etc., $\Delta\tau$ is decreased to half of its previous value. All data presented in this study were obtained from the computer of IBM Model 360 at the RPI Computer Laboratory.

Table 2 Sensitivity of solutions to the number of A_m used
($H_s = 1.2$, $\bar{a} = 0.312$, $F = 10{,}000$, $W = \infty$)

Number of A_m used	H_c
4	0.909
5	0.892
6	0.889
7	0.882

IV. Results and Discussions

Verification from Experimental Data

It is felt that one way to verify the validity of computed results and the methods used in this study is to assimilate some experimental tests. To this end, Ref. 3 was chosen for comparison. In this reference, there is a set of photographic data for the free surface at various time events and also the following information: radius ratio of the tank to the drain $r_o/a = 10$, axial velocity of the undistorted free surface $V_m = 4.2$ in./sec, dimensionless quantity $V_m^2/2ga = 0.233$, maximum distortion of the free surface at $t_c = 0.25$ sec. From this information together with the photographs, the following dimensionless parameters are obtained: $\bar{a} = 0.1$, $H_s = 1.57$, $F = 467$, $\tau_c = 0.665$.

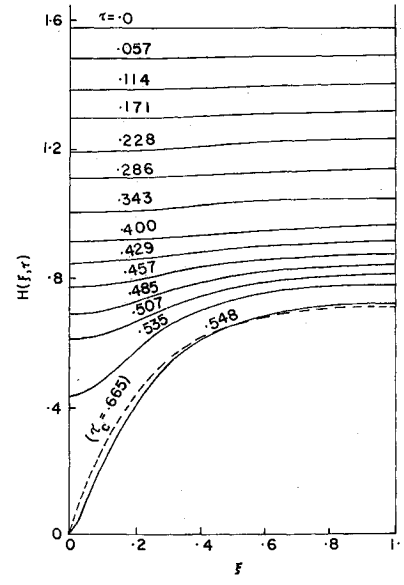

Fig. 2 Free surface profiles at different time τ. $H_s = 1.57$, $\bar{a} = 0.1$, $F = 467$, $W = \infty$. Solid lines are computed; dashed line is experimental results from Ref. 3.

Under the foregoing simulated conditions, with a negligible surface tension, the computer results were obtained from the method described in Sec. III. Figure 2 shows free surface heights vs various radial distances at different times. In the beginning, the entire surface, remaining flat, moves slowly downward at a constant speed until about $\tau = 0.286$. Then, a bulge starts to form in the central portion of the free surface which travels faster than the remaining part of the free surface. Finally, at $\tau = 0.548$, the center of the free surface reaches the drain while the portion near the wall remains essentially flat at a critical height of 0.710. The aforementioned experimental data is also plotted in the same figure for comparison. The latter shows the dip formation at a critical time $\tau_c = 0.665$ with a critical height of 0.695. The agreements can be regarded as reasonable.

Reference 3 also gives numerous experimental data on the critical heights for different drain sizes, fluids, initial heights and dimensionless parameters, $V_m^2/2ag$. These data points are reproduced and plotted in Fig. 3 with respect to the same dimensionless parameter as previously defined. There are also computer results from this study shown in the same figure for comparison. It is seen that those computed results agree with experiments quite well, particularly so in the high dimensionless parameter region. Reference 3 also has the data corresponding to very small $V_m^2/(2ag)$. However, in view of the excessive computational time needed, we stopped our computation at the value of 0.1.

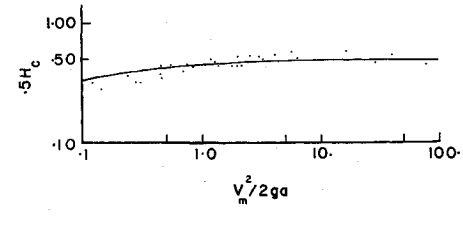

Fig. 3 Comparison of computed results (solid line, based on $H_s = 1.2$, $\bar{a} = 0.312$, $W = \infty$) and experimental data (dots taken from Ref. 3).

Effects of Initial Height, Drain Size, Froude Number, and Weber Number

Figure 4 shows the effect of the initial height on the critical height. It is interesting to note that 1) H_c reaches a constant

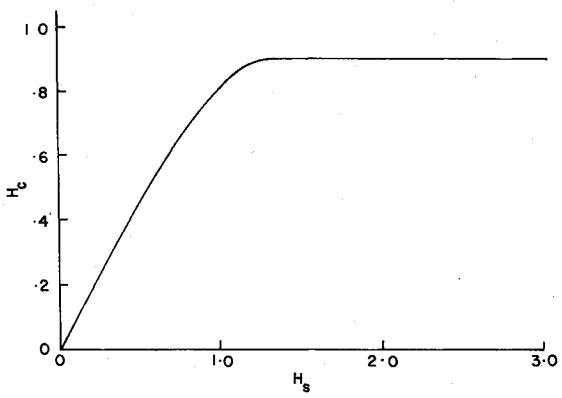

Fig. 4 Dimensionless critical-height vs dimensionless initial-height; $\bar{a} = 0.312$, $F = 10^4$, $W = \infty$.

value of 0.9 when H_s is above 1.2 and 2) $H_s \approx H_c$ when H_s is below 0.5. Figure 5 shows histories of $H(0,\tau)$ for various $\bar{a}$'s. For smaller drain sizes, less discharge before the dip formation is evident. For larger $\bar{a}$'s, however, those which enable a greater discharge, a constant slope dominating a major part of the flow is seen. It can be shown that the free surface in the case of $\bar{a} = 1$ will move downward as expressed below

$$h(\xi, \tau) = H_s(1 - \tau) \tag{28}$$

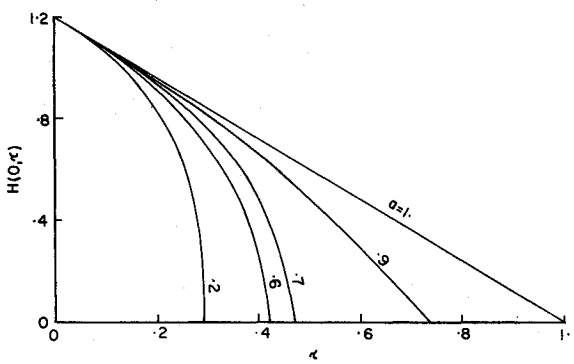

Fig. 5 Histories of dimensionless central-height of free surface for various drain sizes: $H_s = 1.2$, $F = 10^4$, $W = \infty$.

At $\tau = 1$, the entire free surface reaches the bottom of the tank. Figure 6 shows free surfaces at critical flow for various $\bar{a}$'s.

The effect of the Froude number F can be seen from Fig. 3. We note that τ_c decreases as F_v increases and approaches a constant value of 0.92 for large F_v. In the low F_v region there exists a critical Froude number which was determined experimentally by Harleman et al.[4] for a two-layer stratified fluid system as

$$F_{cr} = Q_c/(g'h_c^5)^{1/2} = 0.51\,\pi \tag{29}$$

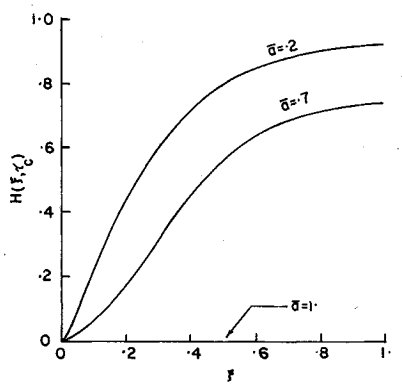

Fig. 6 Free surface profile at critical flow for various drain sizes. $H_s = 1.2$, $F = 10^4$, $W = \infty$.

From the result at the low F_v, say $F_v = 0.467$, of Fig. 3 for a case of upper fluid much lighter than that of the lower one, we find that $\bar{F}_{cr}$ computed has an identical value of $0.51\,\pi$. As far as the influence from the Weber number is concerned, Figs. 7 and 8 show the similar kind of effect on the drainage characteristics as that from the Froude number. No study is made for low Weber numbers since the contact angle is taken to be 90° throughout the present paper.

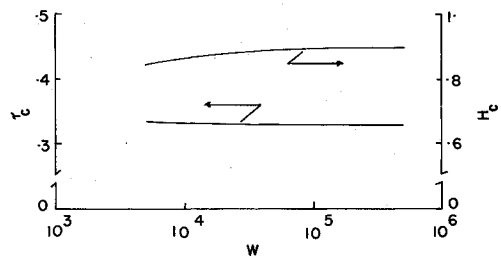

Fig. 7 Dimensionless critical height and dimensionless time for various Weber numbers. $H_s = 1.2$, $\bar{a} = 0.312$, $F = 10^4$.

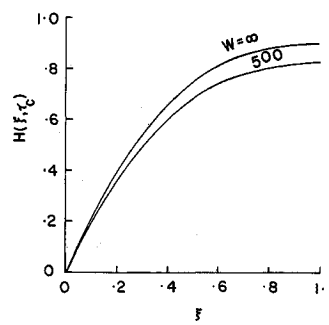

Fig. 8 Comparison of free surface profiles at critical flow, with and without surface tension. $H_s = 1.2$, $\bar{a} = 0.312$, $F = 10^4$.

Remarks on the Results of Ref. 1

In this section, we compare the results of Easton and Catton with those obtained by the method of the present paper. The cases which they computed are based on $W_e/\bar{a} = 6.0$ and $B_o = 100$, where $W_e = 2\rho r_o V_m^2/T$ (Weber number), $B_o = \rho g(2r_o)^2/T$ (Bond number) and $V_m = U\bar{a}^2$ (average velocity in the tank). Other symbols appearing above are the same as those previously defined in this study. They have shown central-height ratios vs time parameter, defined as $\bar{t} = t(\rho r_o^3/T)^{-1/2}$, for various initial-height ratios ranging from $H_s = 0.3$ to 0.48. In addition to the given data, the dimensionless drain size $\bar{a}$ is measured and computed as $\bar{a} = 0.111$. Hence, comparable input data for the present computer program are calculated as the following:

$$W = r_o\rho U^2/(T) = (W_e/\bar{a})\bar{a}^{-3}/(2) = 6/2 \times (0.111)^{-2} = 2200$$

and

$$F = U^2/(gr_o) = 4W/(B_o) = (4 \times 2200)/100 = 88$$

The dimensionless time is also converted into their time parameter by the following identity:

$$\bar{t} = t/(\rho r_o^3/T)^{1/2} = \tau H_s/(\bar{a}^2 W^{1/2})$$

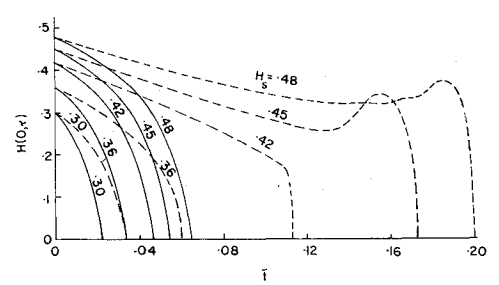

Fig. 9 Comparison of histories of dimensionless central height of free surface for various dimensionless initial heights. Solid lines are present results, dashed lines are results of Ref. 1.

Figure 9 shows the comparison of time-history curves of central-height ratios between the results obtained by the present study and those from Easton and Catton which are respectively represented by the solid lines and the dash lines. It is seen that first, for the same initial-height ratio, the solid lines indicate much smaller critical time parameters than those dash lines. In other words, the present study predicts a much earlier inception of a dip formation and consequently, more residue volume at the critical flow than those from Ref. 1. This information is listed in Table 3 for convenience.

Table 3 Comparison of characteristics at critical flow between the present study and Ref. 1 ($\bar{a} = 0.11$, $W_e/\bar{a} = 6.0$, $B_o = 100.00$)

	Critical time parameter		Fractional residue volume	
H_s	Present study	Ref. 1	Present study	Computed from Ref. 1
0.30	0.022	0.033	0.96	0.94
0.36	0.033	0.060	0.95	0.90
0.42	0.047	0.113	0.94	0.84
0.45	0.055	0.173	0.93	0.78
0.48	0.065	0.200	0.92	0.76

Secondly, all curves from the present study show monotonically decreasing slopes, whereas in Ref. 1, the curves with $H_s = 0.48$ and 0.45 show a reversal of the central velocity. Easton and Catton explained this reversal on the basis of surface oscillations induced by the drain. However, any surface oscillations associated with the sudden opening of the drain are due mainly to the pressure waves originated at the drain which can hardly be expected to be described by the model of incompressible fluid under the boundary conditions of uniform drain velocity at all times.

Thirdly, the initial rates of decrease of the free surface at the center line are much steeper from the present study than those from Ref. 1. A thorough discussion appears in the Appendix.

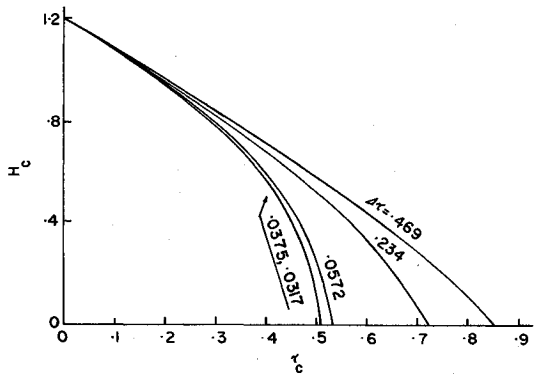

Fig. 10 Sensitivity of central-height history to the choices of initial $\Delta\tau$. $H_s = 1.2$, $\bar{a} = 0.75$, $F = 10^4$, $W = \infty$.

Appendix: Initial Rate of Decrease of the Free Surface Height

When the drain is just open, $\tau = 0$, the potentials at any point are constant and are taken to be zero. In conjunction with an initially flat free surface, we have

$$\varphi(\xi, H_s) = 0 \quad \text{at } \tau = 0 \tag{A1}$$

Thus, the components of the axial velocity may be obtained, from Eq.(19), in a closed form,

$$\left.\frac{\partial\varphi(\xi,\eta)}{\partial\eta}\right|_{\eta=H_s,\tau=0} = -\bar{a}^2 + \sum_{m=1}^{\infty} \frac{-2\bar{a}J_1(k_m\bar{a})J_0(k_m\xi)}{k_m J_0^2(k_m)\cosh(k_m H_s)} \tag{A2}$$

We note that the initial components of the axial velocity depends on the geometrical parameters H_s and $\bar{a}$ and cannot be arbitrarily prexcribed. By virtue of $\partial\varphi(\xi,\eta)/\partial\xi = \partial h(\xi,\eta)/\partial\xi = 0$, $\eta = H_s$ and $\tau = 0$, the initial rate of decrease of the free surface height can be obtained by substituting Eq. (A2) into Eq. (3) or

$$h_\tau(\xi,\tau)\Big|_{\tau=0^+} = \left[-\bar{a}^2 - \sum_{m=1}^{\infty} \frac{2\bar{a}J_1(k_m\bar{a})J_o(k_m\xi)}{k_m J_o^2(k_m)\cosh(k_m H_s)}\right] H_s\bar{a}^{-2} \tag{A3}$$

Equation (A3) indicates that the initial rate of decrease of the free surface height depends only on the geometrical parameters H_s and $\bar{a}$. In the center where $\xi = 0$ and $J_o(0) = 1$, Eq. (A3) becomes

$$h_\tau(\xi,\tau)\Big|_{\substack{\xi=0\\\tau=0}} = \left[-\bar{a}^2 - \sum_{m=1}^{\infty} \frac{2\bar{a}J_1(k_m\bar{a})}{k_m J_o^2(k_m)\cosh(k_m H_s)}\right] H_s\bar{a}^{-2} \tag{A4}$$

which can be expressed in terms of the time parameter $\bar{t}$ of Ref. 1, as

$$\left.\frac{\partial h(\xi,\bar{t})}{\partial\bar{t}}\right|_{\substack{\xi=0\\\bar{t}=0}} = \left[-\bar{a}^2 - \sum_{m=1}^{\infty} \frac{2\bar{a}J_1(k_m\bar{a})}{k_m J_o^2(k_m)\cosh(k_m H_s)}\right] W^{1/2} \tag{A5}$$

For the typical cases as mentioned in Sec. IV, these initial rates of the decrease of the free surface height at the center line are both computed from Eq. (A5) and measured graphically from Fig. 9. The results from both this study and Ref. 1 are listed in Table 1 for comparison. It is seen that results from the present study agree quite well with those computed values from Eq. (A5), while those from Ref. 1 are less steep by 23% to 32%.

References

[1] Easton, C. R. and Catton, I., "Nonlinear Free Surface Effects in Tank Draining at Low Gravity," *AIAA Journal*, Vol. 8, No. 12, Dec. 1970, pp. 2195–2206.

[2] Saad, M. D. and Oliver, D. A., "Linearized Time-Dependent Free Surface Flow in Rectangular and Cylindrical Tanks," *Proceedings of the 1964 Heat Transfer and Fluid Mechanics Institute*, June 1964, pp. 81–99.

[3] Gluck, D. F., Gille, J. P., Zukoski, E. E., and Simpkin, D. J., "Distortion of the Liquid Surface during Tank Discharge," *Journal of Spacecraft and Rockets*, Vol. 3, No. 11, Nov. 1966, pp. 1691–1692.

[4] Harleman, D. R. F., Morgan, R. L., and Purple, R., "Selective Withdrawal from a Vertically Stratified Fluid," *Proceedings 8th Congress of the International Association for Hydraulic Research*, Canada, Aug. 1959, pp. 10-C-1–10-C-16.